Implications of the cardiomyocyte stress response on protein homeostasis in atrial fibrillation

Wiersma, Marit

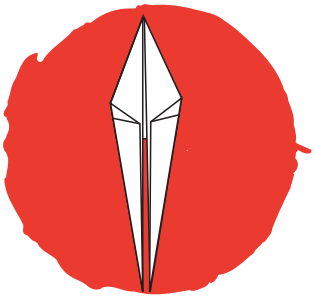

Chapter 6

The orphan drug 4-phenyl butyrate protects the heart against Atrial Fibrillation by blocking ER stress-induced autophagy

Marit Wiersma[1*], Roelien A.M. Meijering[1*], XiaoYan Qi[2], Deli Zhang[1], Tao Liu[2], Femke Hoogstra-Berends[1], Ody C.M. Sibon[3], Robert H. Henning[1], Stanley Nattel[2], Bianca J.J.M. Brundel[1,4]

[1]Department of Clinical Pharmacy and Pharmacology, University Medical Center Groningen, University of Groningen, The Netherlands.
[2]Department of Medicine, Montreal Heart Institute and Université de Montréal and the Department of Pharmacology and Therapeutics, McGill University, Montreal, Québec, Canada.
[3]Department of Cell Biology, University Medical Center Groningen, University of Groningen, The Netherlands.
[4]Department of Physiology, Institute for Cardiovascular Research, VU University Medical Center, Amsterdam, The Netherlands.

*Contributed equally

Submitted

ABSTRACT

Derailment of proteostasis, the homeostasis of production, function and breakdown of proteins, contributes importantly to the self-perpetuating nature of atrial fibrillation (AF), the most common heart-rhythm disorder in man. Autophagy plays a key role in proteostasis by degrading protein aggregates and aberrant proteins and damaged or old organelles. Here, we report that tachycardia, induced by rapid pacing in cardiomyocytes, *Drosophila* and dogs, activates autophagy as an event downstream of endoplasmic reticulum (ER) stress. Blocking ER stress by the chemical chaperone 4-phenyl butyrate prevents activation of autophagy and forestalls cardiomyocyte damage, contractile dysfunction and AF progression in these models, both *in vitro* and *in vivo*. Moreover, overexpression of the ER chaperone-protein HSPA5 or treatment with inhibitors of autophagy (bafilomycin A1, pepstatin A) confirms involvement of the ER stress-induced autophagy pathway in derailing cardiomyocyte function. Atrial cells from patients with persistent AF also show induction of ER stress and activation of autophagy, which correlates with markers of cardiomyocyte damage (cardiac troponins, α-tubulin and myolysis). Together, these results identify ER stress-induced autophagy as a major pathway in the progression of AF and demonstrate the therapeutic action of a currently marketed inhibitor of ER stress, 4-phenyl butyrate.

INTRODUCTION

Atrial fibrillation (AF) is the most common persistent clinical tachyarrhythmia, provoked by increased atrial activation rate due to the existence of re-entry circuits.[1] Not only do many patients suffer from clinical symptoms, including palpitations, fatigue and weakness, AF also puts patients at considerable risk for cardiac morbidity and mortality and often necessitates life-long anticoagulant therapy.[1] Once the arrhythmia occurs, sinus rhythm reversion and maintenance becomes progressively more difficult. Central to this self-perpetuating nature of AF is the remodeling of cardiomyocytes as a consequence of the increased atrial activation rate, resulting in disturbances of electrophysiology and contraction.[2] Therapeutic strategies that limit cardiomyocyte remodeling would improve the success of cardioversion, but are currently unavailable.[1] To identify druggable targets, recent research is increasingly directed at uncovering the underlying molecular mechanisms that are key to cardiac remodeling.

Derailment of proteostasis, i.e. the homeostasis of protein production, function and breakdown, contributes importantly to cardiomyocyte remodeling and predisposes to AF in experimental models and AF patients.[3-6] Amongst the recently identified factors contributing to derailment of proteostasis in AF are the activation of proteases and degradation of contractile and structural proteins, including cardiac troponins and α-tubulin, resulting in breakdown of the microtubule network and structural remodeling.[3,4,7] The importance of proper proteostasis is also unveiled by the attenuation of cardiomyocyte remodeling and dysfunction via the induction of heat shock proteins, whose chaperone function serves correct folding of proteins and preservation of contractile proteins.[8,9]

Macroautophagy (hereafter 'autophagy') is critically involved in maintaining proteostasis.[10] Autophagy is an evolutionarily conserved protein degradation pathway that removes damaged or expired proteins and organelles by sequestration in autophagosomes and subsequent lysosomal degradation.[10,11] Recent work suggests that the autophagy–lysosome pathway plays a major role in the cardiac stress response.[12] Autophagy is widely involved as a cell-stress pathway, whose excessive activation may trigger cardiac remodeling in response to degradation of essential proteins and organelles. Activation of autophagy in the heart is implicated in cardiac remodeling in mitral regurgitation[13,14] and cardiac hypertrophy.[15]

Here, we report that activation of autophagy by upstream endoplasmic reticulum (ER) stress constitutes an important mechanism of cardiac remodeling in rapidly paced cardiomyocytes, *Drosophila* and dogs, and in atrial biopsies from AF patients.

We provide data to show that blocking ER stress, by the chemical chaperone 4-phenyl butyrate, inhibits activation of autophagy, and thereby precludes electrical and contractile dysfunction in both *in vitro* and *in vivo* AF models. Thus, our study points to a novel therapeutic option to attenuate cardiac remodeling in AF, by use of the currently marketed inhibitor of ER stress, 4-phenyl butyrate.

MATERIALS AND METHODS

HL-1 atrial cardiomyocyte cell culture, transfections and constructs

HL-1 atrial cardiomyocytes, derived from adult mouse atria, were obtained from Dr. William Claycomb (Louisiana State University, New Orleans, USA).[16] The cardiomyocytes were maintained in complete Claycomb Medium (Sigma, The Netherlands) supplemented with 10% FBS (PAA Laboratories GmbH, Austria), 100 U/ml penicillin (GE Healthcare, The Netherlands), 100 µg/ml streptomycin (GE Healthcare, The Netherlands), 4 mM L-glutamine (Gibco, The Netherlands), 0.3 mM L-ascorbic acid (Sigma, The Netherlands) and 100 µM norepinephrine (Sigma, The Netherlands). HL-1 cardiomyocytes were cultured on cell culture plastics or on glass coverslips coated with 0.02% gelatin (Sigma, The Netherlands) in a humidified atmosphere of 5% CO_2 at 37°C. Where indicated, HL-1 cardiomyocytes were transiently transfected with the LC3B-GFP (kind gift of Prof. T. Johansen),[17] HSPA5 (kind gift of Prof. H. Kampinga) or pcDNA3.1+ (empty) plasmid, by the use of Lipofectamin 2000 (Life Technologies, The Netherlands).

Tachypacing of HL-1 cardiomyocytes and calcium transient measurements

HL-1 cardiomyocytes were subjected to tachypacing as described before.[3] In short, HL-1 cardiomyocytes were subjected to 1Hz (normal pacing) or 6Hz (tachypacing), 40V and 20ms pulses, for a duration of maximal 8 hours via the C-Pace100TM-culture pacer (IonOptix Corporation, The Netherlands). To measure calcium transients (CaT), HL-1 cardiomyocytes were incubated for 30 min with 2 µM of the Ca^{2+}-sensitive Fluo-4-AM dye (Invitrogen, The Netherlands), followed by 3 times washing with DMEM (Gibco, The Netherlands). Fluo-4 loaded cardiomyocytes were excited by a 488 nm laser with emission at 500-550 nm and were visually recorded with a 40x-objective, using a Solamere-Nipkow-Confocal-Live-Cell-Imaging system (based on a Leica DM IRE2 inverted microscope). The live recording of CaT in HL-1 cardiomyocytes was performed

at 1Hz stimulation at 37°C. Live recordings were further processed by use of the software ImageJ (National Institutes of Health, USA). The relative value of fluorescent signals between experiments was determined utilizing the following calibration: Fcal=F1/F0, where F1 is the fluorescent dye signal at any given time and F0 is the fluorescent signal at rest. Mean values and SEM from each experimental condition were based on 7 consecutive CaT in at least 50 cardiomyocytes.

Drosophila stocks, tachypacing and heart wall contraction assays

For all experiments w^{1118} strains were used. All flies were maintained at 25°C on standard medium. After fertilization, adult flies were removed and drugs were added to the medium containing fly embryos. *Drosophilas* were treated with 4-phenyl butyrate (4PBA, 100 mM), pepstatin A (100 μM) or bafilomycin A1 (100 nM). Controls were treated with the vehicle 2% DMSO. After 2 days, prepupae were selected for tachypacing, as previously described.[3] Groups of at least 5 pupae were subjected to tachypacing (5Hz for 20 minutes, 20V and 5ms pulses) with a C-Pace100TM-culture pacer (IonOptix Corporation, The Netherlands). Before and after tachypacing, movies of spontaneous heart wall contractions in whole pupae were recorded for 30 seconds. Heart wall contractions were analyzed with IonOptix software.

Drug treatment

Pepstatin A, bafilomycin A1 and 4PBA were purchased from Sigma (The Netherlands) and dissolved according to manufacturer's instructions. HL-1 cardiomyocytes were treated with 4PBA (10 mM) 8 hours prior to pacing. Pepstatin A (10 μM) and bafilomycin A1 (10 nM) were added 30 minutes prior to normal or tachypacing.

Antibodies and reagents

Antibodies were purchased from the following vendors: rabbit monoclonal anti-phospho-Akt (Ser473, #4060), rabbit monoclonal anti-Akt (#4691), rabbit polyclonal anti-LC3B (#2775), rabbit polyclonal anti-SQSTM1/p62 (#5114), rabbit polyclonal anti-phospho-eIF2α (Ser51, #9721), rabbit monoclonal anti-phospho-S6 Ribosomal Protein (Ser235/236, #4858), mouse monoclonal anti-S6 Ribosomal Protein (#2317), rabbit polyclonal anti-phospho-mTOR (Ser2448, #2971), rabbit polyclonal anti-phospho-mTOR (Ser2481, #2974), rabbit monoclonal anti-mTOR (#2983, all Cell Signaling Technology, The Netherlands), mouse monoclonal anti-eIF2α (ab5369, Abcam, UK), mouse monoclonal anti-HSPA5 (ab21685, Abcam, UK), mouse monoclonal anti-β-actin

(# sc47778, Santa Cruz Biotechnology, USA) and mouse monoclonal anti-GAPDH (#10R-G109a, Fitzgerald, USA). Horseradish peroxidase-conjugated anti-mouse or anti-rabbit (Dako, Denmark) were used as secondary antibodies.

Western blot analysis

Western blot analysis was performed as previously described.[3] Briefly, equal amounts of total protein in SDS-PAGE sample buffer were separated on SDS-PAGE 4-20% PreciseTM Protein gels (Thermo Scientific, The Netherlands). After transfer to nitrocellulose membranes (Stratagene, The Netherlands), membranes were incubated with primary antibodies, followed by incubation with horseradish peroxidase-conjugated secondary antibodies. Signals were detected by the Western Lightning Ultra (PerkinElmer, USA) method and quantified by densitometry via the software Gene Gnome, Gene tools (Syngene, Cambridge, UK).

Quantitative RT-PCR

Total RNA was isolated from HL-1 cardiomyocytes utilizing the nucleospin RNA isolation kit (Machery-nagel, The Netherlands). First-strand cDNA was generated by M-MLV reverse transcriptase (Promega, The Netherlands) and random hexamer primers (Promega, The Netherlands). Relative changes in transcription level were determined using the CFX384 Real-time system C1000 Thermocycler (Bio-Rad, The Netherlands) in combination with SYBR green ROX-mix (Westburg, The Netherlands). Calculations were performed using the comparative CT method according to User Bulletin 2 (Applied Biosystems, The Netherlands). Fold inductions were adjusted for GAPDH levels.
Primer pairs used included: ATF4 fw: GTCCGTTACAGCAACACTGC and rv: CCACCATGGCGTATTAGAGG, ATF6 fw: AAGAGAAGCCTGTCACTG and rv: GGCTGGTAGTGTCTGAAT, CHOP fw: GACCAGGTTCTGCTTTCAGG and rv: CAGCGACAGAGCCAGAATAA, HSPA5 fw: ATCTTTGGTTGCTTGTCGCT and rv: ATGAAGGAGACTGCTGAGGC, ATG12 fw: CTCCACAGCCCATTTCTTTG and rv: AACTCCCGGAGACACCAAG and GAPDH fw: CATCAAGAAGGTGGTGAAGC and rv: ACCACCCTGTTGCTGTAG. PCR efficiencies for all primer pairs were between 90-110%.

Immunofluorescent staining and confocal analysis

HL-1 cardiomyocytes were untransfected or transiently transfected with GFP-LC3B for 48 hours and paced at 1Hz (normal pacing) or 6Hz (tachypacing), followed by fixation with 4% formaldehyde (Klinipath, The Netherlands) for 15 minutes at room temperature,

washing three times with phosphate buffered saline (PBS), permeabilized and blocked with 0.3% triton-X100 and 5% FBS in PBS (1h room temperature). Endogenous LC3B was visualized by the anti-LC3B antibody and a secondary Alexa-488 labeled anti-rabbit antibody (Invitrogen, The Netherlands) and endogenous myosin heavy chain (MHC) was visualized by the anti-MHC antibody (kind gift of Prof. J. Van der Velden) and a secondary FITC labeled anti-rabbit antibody (Southern Biotech, USA). Endogenous LC3B, GFP-LC3B puncta, indicative of autophagosomes, and MHC were visualized by confocal microscopy (Leica TCS SP8) and captured at 125x magnification. The number of puncta was counted manually from at least two independent experiments using imagePro. Mean values and SEM from each experimental condition were based on at least 20 cardiomyocytes in case of transfection and at least 200 in case of drug treatment.

Dog in vivo model for AF

Dogs were anesthetized with acepromazine (0.07 mg/kg i.m.), ketamine (5.3 mg/kg i.v.), diazepam (0.25 mg/kg, i.v.) and isoflurane (1.5%), intubated and ventilated. One bipolar pacing lead was fixed into the right atrial (RA) appendage via the left jugular vein under fluoroscopic guidance. The tip was connected to a programmable pacemaker (Star Medical, Japan). Results in 7 atrial tachypaced dogs with Na-PBA were compared with 7 tachypaced dogs without treatment and 7 non-paced control dogs. Na-PBA (Scandinavian Formulas USA, obtained via EM-Partners AB, Sweden) was given orally (300 mg/kg per day), starting 3 days before and continuing throughout atrial tachypacing. For ATP and ATP + Na-PBA groups, the pacemakers were turned on 24 hours after surgery to stimulate the RA at 600 bpm for 7 successive days. The ECG was checked daily to ensure AF during pacing. At the end of the study, all dogs were anesthetized with morphine (2mg/kg s.c.) and α-chloralose (120 mg/kg i.v. bolus followed by 29.25 mg/kg/hr i.v. infusion), intubated and ventilated. Body temperature was maintained at 37°C. After midline sternotomy, the pericardium was opened and 2 bipolar electrodes were fixed to the RA appendage (one for pacing, one for signal recording). For AF induction, the RA was paced at 50Hz for 10 seconds. A total of 5-10 AF episodes were recorded to calculate the mean AF duration in each dog. An AF episode >10 minutes was considered sustained, and the electrophysiological study was terminated. Cardioversion was avoided to prevent tissue damage, which precludes further cellular and molecular studies.

Atrial cardiomyocyte isolation

After electrophysiological study, the heart was excised and immersed in oxygen-saturated Tyrode solution: 136 mM NaCl, 5.4 mM KCl, 1 mM $MgCl_2$, 2 mM $CaCl_2$, 0.33 mM NaH_2PO_4, 5 mM HEPES and 10 mM dextrose, pH 7.35 by NaOH. The left atrium (LA) was isolated from the heart with intact blood supply. The left circumflex coronary artery was cannulated and perfused with Ca^{2+} (1.8 mM) followed by Ca^{2+}-free Tyrode-solution perfusion for 10 minutes. All leaking branches were ligated. The tissue was then perfused with Ca^{2+}-free Tyrode-solution containing 150 U/mL collagenase (Worthington, type II) and 0.1% bovine serum albumin (BSA) for 60 minutes. Digested LA tissue was harvested and carefully stirred. Isolated cells were centrifuged (500 rpm, 3 minutes) to separate cardiomyocytes from fibroblasts. Cardiomyocytes were stored in Tyrode-solution containing 200 µmol/L Ca^{2+} for Ca^{2+}-imaging studies.

Cardiomyocyte Ca2+ imaging and cellular contractility assessment

Isolated cardiomyocytes were stimulated at 1Hz and all measurements were performed at 35±2°C. Cell-Ca^{2+} recording was obtained as previously described with the use of Indo-1 AM.[3,8] Cells were exposed to UV light (wavelength 340 nm) and the exposure was controlled with an electronic shutter to minimize photo bleaching. Emitted light was reflected into a spectral separator, passed through parallel filters at 400 and 500 nm (±10 nm), detected by matched photomultiplier tubes and electronically filtered at 60Hz. Background fluorescence was removed by adjusting the 400 and 500 nm channels to 0 over an empty field of view near the cell. Fluorescence signal ratios (R) were recorded and converted to $[Ca^{2+}]i$ following the equation developed by Grynkiewicz et al.:[18] $[Ca^{2+}]i = K_d\beta [(R - R_{min})/(R_{max} - R)]$ where β is the ratio of the 500 nm signals at very low and saturating $[Ca^{2+}]i$. Intracellular Kd for Indo-1 was 844 nm. Cell and sarcomere contractility was detected by automatic edge-detection and 5 successive beats were averaged for each measurement.

Cell Electrophysiology Recordings

Borosilicate glass electrodes (Sutter Instruments, USA) filled with pipette solution were connected to a patch-clamp amplifier (Axopatch 200A, Axon Instruments, USA). Electrodes had tip resistances of 2-4 MΩ. For perforated-patch recording, nystatin-free intracellular solution was placed in the tip of the pipette by capillary action (~30 seconds), then pipettes were back-filled with nystatin-containing (600

µg/mL) pipette solution. Data were sampled at 5kHz and filtered at 1kHz. Whole cell currents are expressed as densities (pA/pF). Junction potentials between bath and pipette solutions averaged 10.5 mV and were corrected for APs only. Tyrode's solution contained: 136 mM NaCl, 1.8 mM $CaCl_2$, 5.4 mM KCl, 1 mM $MgCl_2$, 0.33 mM NaH_2PO_4, 10 mM dextrose and 5 mM HEPES, titrated to pH 7.3 with NaOH. The pipette solution for AP-recording contained: 0.1 mM GTP, 110 mM potassium-aspartate, 20 mM KCl, 1 mM $MgCl_2$, 5 mM MgATP, 10 mM HEPES, 5 mM sodium-phosphocreatine and 0.005 mM EGTA (pH 7.4, KOH). The extracellular solution for Ca^{2+}-current (ICa) measurement contained: 136 mM tetraethylammonium-chloride, 5.4 mM CsCl, 1 mM $MgCl_2$, 2 mM $CaCl_2$, 0.33 mM NaH_2PO_4, 10 mM dextrose and 5 mM HEPES (pH 7.4, CsOH). Niflumic acid (50 µM) was added to inhibit Ca^{2+} dependent Cl current, and 2 mM 4-aminopyridine to suppress Ito. The pipette solution for ICa-recording contained 120 mM CsCl, 20 mM tetraethylammonium-chloride, 1 mM $MgCl_2$, 10 mM EGTA, 5 mM Mg-ATP, 10 mM HEPES and 0.1 mM Li-GTP (pH 7.4, CsOH).

Patient material

Prior to surgery, one investigator assessed patient characteristics (Table 1) as described before.[7] All patients were euthyroid and had normal left ventricular function. Coumarin therapy was interrupted 3 days before surgery. Right and left atrial appendages (RAA and LAAs, respectively) were obtained from all patients. After excision, the atrial appendages were immediately snap frozen in liquid nitrogen and stored at -85ºC. The study conforms to the principles of the Declaration of Helsinki. The institutional review board approved the study and patients gave written informed consent.

Statistical analysis

Results are expressed as mean ± SEM of at least three independent experiments. Multiple-group comparisons were done with one-way ANOVA with a Bonferroni correction. Correlation was determined using the Spearman correlation test. All P-values were two-sided. A value of $P \leq 0.05$ was considered statistically significant. SPSS version 20 was used for all statistical evaluations.

RESULTS

Tachypacing of cardiomyocytes induces autophagy

To explore whether tachypacing induces autophagy, selective autophagy markers were tested, including p62 and LC3B. P62 is sequestrated to autophagosomes during autophagy and degraded upon fusion with the lysosome; its levels are inversely

Table 1 Demographic and clinical characteristics of patients with paroxysmal AF (PAF), patients with persistent AF (PeAF) and control patients in sinus rhythm (SR).

	SR	PAF	PeAF
N	6	6	7
RAA (n)	6	6	6
LAA (n)	4	6	5
Age (years)	56±8	51±7	61±10
Duration of AF (median, range (months))	-	-	14.6 (8-56)
Underlying heart disease (n)			
CAD/MVI	6	7	7
New York Health Association for exercise tolerance			
I	3	5	3
II	3	2	4
Echocardiography			
Left atrial diameter (parasternal)	42±3	42±4	48±4
Left ventricular end-diastolic diameter (mm)	50±4	52±3	52±3
Left ventricular end-systolic diameter (mm)	34±4	38±3	34±5

Values are represented as mean ± SEM or number of patients. CAD: coronary artery disease, MVI: mitral valve insufficiency.

proportional to activation of autophagy.[19,20] LC3B-II is a protein produced from LC3B-I upon activation of autophagy and is also incorporated into autophagosomes: LC3B-II levels are proportional to the number of autophagosomes.[19,20] Tachypacing of HL-1 atrial cardiomyocytes activates autophagy, as demonstrated by a time-dependent decrease in the expression of p62, and increase in LC3B-II (Figure 1A-C). Tachypacing also induces a clear redistribution of LC3B into discrete perinuclear puncta in both untransfected cardiomyocytes and LC3B-GFP transfected cardiomyocytes (Figure 1D-F), supporting autophagosome formation.[21] Next, we determined the autophagic flux, to discriminate between the induction of autophagy and decreased degradation of autophagosomes, by blocking autophagosome-lysosome fusion with bafilomycin A1 (BAF, Figure 1G and H).[22] BAF pretreatment further increases LC3B-II levels of tachypaced cardiomyocytes (Figure 1G and H and S1), indicating that tachypacing activates autophagy in HL-1 atrial cardiomyocytes.

ER stress activates autophagy in cardiomyocyte model and patients with AF

To investigate upstream pathways activating autophagy, we first examined the mammalian target of rapamycin (mTOR). mTOR assembles into two complexes, mTOR complex 1 (mTORC1) and complex 2 (mTORC2), and both complexes become activated by mTOR phosphorylation, although at different sites, after which they

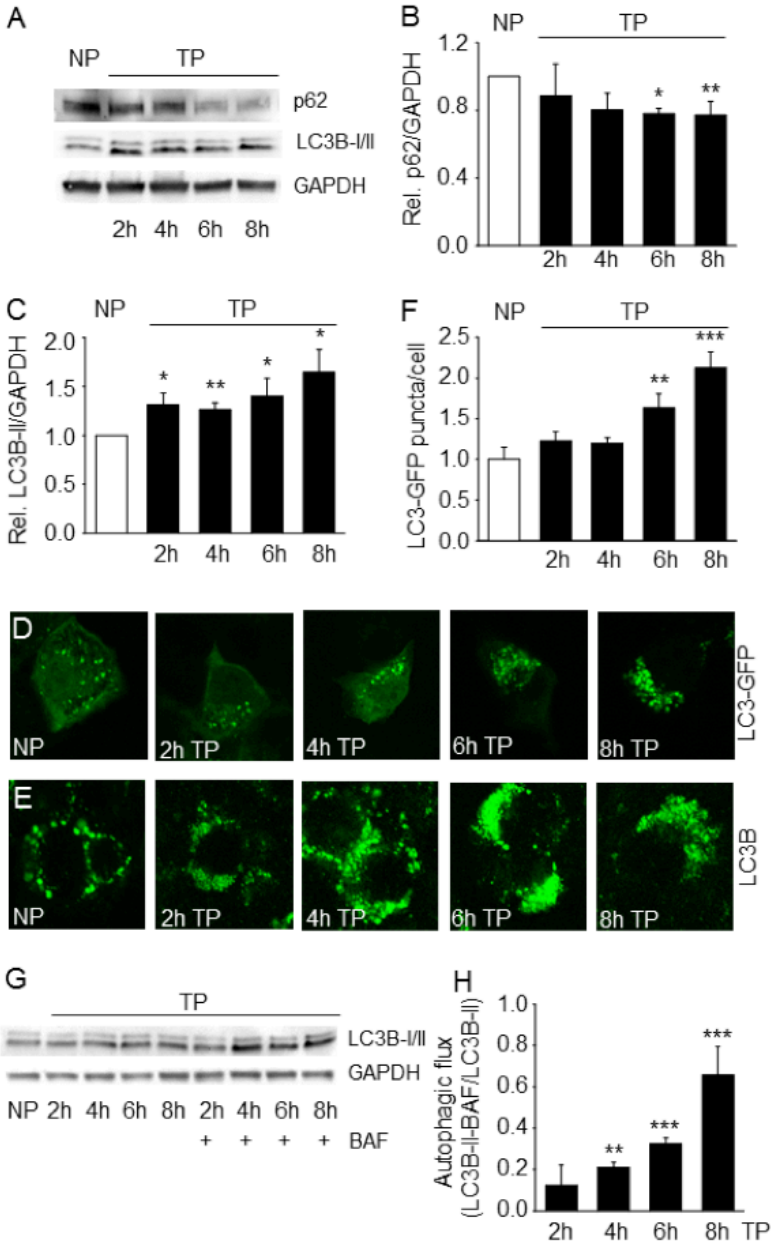

Figure 1 Tachypacing induces autophagosome formation and activation of autophagy. A) Representative Western blot of tachypacing-induced autophagy markers p62, LC3B-I and LC3B-II and loading control GAPDH. HL-1 cardiomyocytes were normal paced (NP) or tachypaced (TP) for the duration as indicated. **B)** Quantified data showing a significant reduction in p62 levels after 6 hours of TP. **C)** Quantified data showing a significant increase in LC3B-II levels after 2 hours of TP. **D)** Confocal images of tachypaced HL-1 cardiomyocytes, for the period as indicated, transfected with LC3B-GFP plasmid. **E)** Confocal images of tachypaced HL-1 cardiomyocytes for the period as indicated. Endogenous LC3B was visualized by immunostaining. Green puncta indicate autophagosomes. **F)** Quantified data showing accumulation of LC3B-GFP puncta/cardiomyocyte during TP, normalized for normal paced (NP). **G)** Representative Western blot of HL-1 cardiomyocytes NP versus TP for the duration as indicated, in the presence or absence of bafilomycin A1 (BAF). **H)** Quantification of the autophagic flux by determining the difference in LC3B-II levels in the presence versus absence of bafilomycin A1 (BAF). *$P \leq 0.05$, **$P \leq 0.01$, ***$P \leq 0.001$ versus NP.

attenuate autophagy.[23,24] To test whether tachypacing-induced autophagy results from the inhibition of mTOR signaling, we determined total mTOR, phosphorylation of mTOR at S2448 for mTORC1, S2481 for mTORC2 and their respective downstream targets ribosomal protein S6 (S6RP) and Akt (Figure 2A-D). Tachypacing does not affect phosphorylation of mTOR at S2448 or S2481, nor phosphorylation of the mTORC1 downstream effector S6RP at S235-236. However, tachypacing significantly increases phosphorylation of Akt at S473 (Figure 2D). Given the increased Akt phosphorylation, we next examined involvement of endoplasmic reticulum (ER) stress signaling in tachypacing-induced autophagy, as Akt S473 phosphorylation is observed in ER stress[25] and ER stress is an important regulator of autophagy.[11,26] A role of ER stress was suggested by the finding that tachypacing strongly increases phosphorylation of its downstream marker eIF2α (Figure 3A and B) and induces transcription of genes activated by ER stress, i.e. ATF4, ATF6, CHOP, HSPA5 and ATG12 (Figure 3C). In addition, tachypacing gradually induced protein levels of HSPA5 (Figure S2), an endogenous ER chaperone-protein induced by ER stress.[11]

To extend our findings to human AF, we examined ER stress and autophagy in right and left atrial appendages (RAA and LAA, respectively) of patients with paroxysmal (PAF) and persistent AF (PeAF), along with control patients in sinus rhythm (SR). Patients with PeAF showed an accumulation of autophagosomes and the presence of myolysis (degradation of sarcomeres) upon electron microscopic examination, which is absent in SR patients (Figure 4A-D). ER stress and autophagy are further evidenced in LAA of patients with PeAF by decreased levels of HSPA5 and p62 and a trend towards enhanced LC3B-II induction (Figure S3) compared to SR (Figure 4E-G). As observed before,[3,27,28] remodeling was less pronounced in right atrium, as the expression levels of HSPA5 and p62 were similar in RAA of patients with PAF, PeAF and SR, indicating that the activation of autophagy is absent. Previously, we reported on structural remodeling, involving degradation of contractile proteins, in these patients.[4,7] Involvement of autophagy in structural remodeling and AF progression is substantiated by the correlation of p62 expression with cardiac troponin (cTnI and cTnT) and α-tubulin expression in PeAF, PAF and SR patients (Figure 4H-J) and inverse correlation with the amount of myolysis (Figure 4K). Levels of p62 also correlated with HSPA5 levels (Figure 4L), suggesting that an ER stress response is strongly associated with autophagy and AF progression. Taken together, these results denote ER stress-mediated activation of autophagy in a tachypaced cardiomyocyte model as well as in left atrial tissue of patients with persistent AF. The correlation of autophagy markers with degradation of contractile

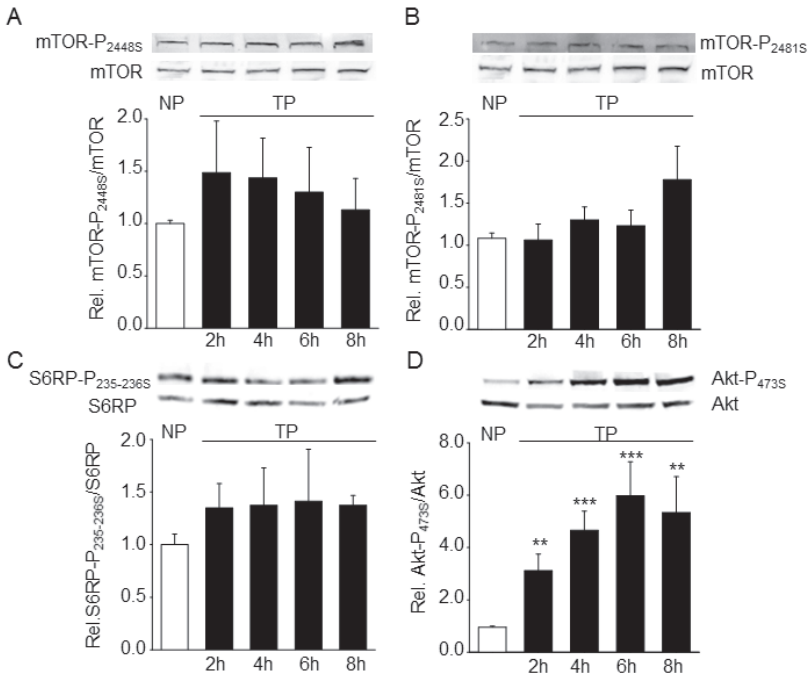

Figure 2 Tachypacing-induced autophagy does not involve mTORC signaling. Top panels represent Western blots of proteins within the mTORC signaling and lower panels reveal quantified data of the ratio phosphorylated proteins normalized for basal protein levels. **A)** Phospho-mTOR 2448S (mTORC1), **B)** Phospho-mTOR 2481S (mTORC2), **C)** Phospho-S6RP 235-236S (downstream of mTORC1) and **D)** Phospho-Akt 473S (downstream of mTORC2 and ER stress) in response to tachypacing (TP) for the duration as indicated compared to normal paced (NP). ***P*≤0.01, ****P*≤0.001 versus NP.

proteins and the amount of structural remodeling suggests a biologically relevant contribution of this pathway to AF-induced derailment of cardiomyocyte proteostasis and disease progression.

Inhibition of ER stress-induced autophagy protects from cardiac remodeling

The orphan drug, 4-phenyl butyrate (4PBA), in clinical use to treat urea cycle disorders,[29-31] has recently been recognized as an inhibitor of ER stress by virtue of its chemical chaperone properties.[32,33] To explore its potential as a therapeutic agent in AF, we examined its properties in tachypaced cardiomyocytes, *Drosophila* and a dog model of AF.

In tachypaced HL-1 cardiomyocytes, 4PBA limits ER stress and prevents activation of autophagy, as demonstrated by a normalization of phospho-eIF2α, attenuation of p62 breakdown and LC3B processing (Figure 5A and B). 4PBA treatment prevents

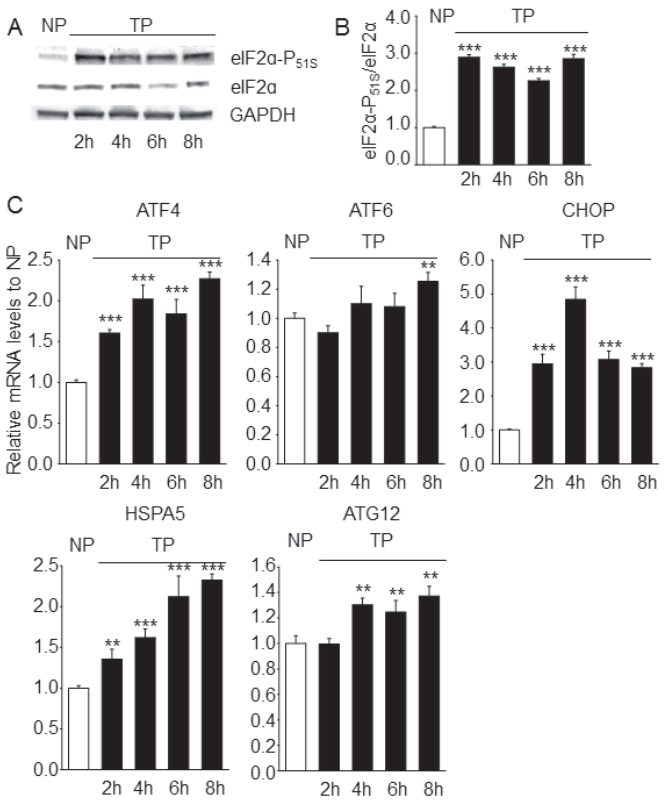

Figure 3 Tachypacing augments levels of ER stress markers and autophagy gene ATG12. A) Representative Western blot of phospho-eIF2α 51S, an ER stress marker, and basal eIF2α and GAPDH levels in response to tachypacing (TP) for the indicated duration or normal pacing (NP). **B)** Quantified data of the ratio phospho-eIF2α 51S normalized for basal eIF2α protein levels. **C)** Quantitative real time PCR of ER stress markers ATF4, ATF6, CHOP and HSPA5 and the autophagy related gene ATG12 in response to tachypacing for the indicated duration relative to normal pacing (NP). ***P*≤0.01, ****P*≤0.001 versus NP.

tachypacing-induced accumulation of the contractile protein myosin heavy chain (MHC) in perinuclear puncta in HL-1 cardiomyocytes (Figure 5C and D). The protective 4PBA effects are mediated via upstream inhibition of autophagy, as downstream inhibition of autophagy by pepstatin A (lysosomal cathepsin D/E inhibitor) or BAF (lysosomal fusion inhibitor) attenuated p62 degradation, but did not affect upstream ER stress, LC3B processing and the formation of perinuclear MHC puncta upon tachypacing (Figure 5A-D). Next, we determined whether 4PBA also blocks tachypacing-induced contractile dysfunction. Pretreatment with 4PBA completely attenuated the loss of calcium transients (CaT) in 8h tachypaced cardiomyocytes (Figure 5E and F and S4). The action of 4PBA is mediated by blocking ER stress-mediated activation of autophagy, as similar effects on CaT were observed in cardiomyocytes overexpressing the endogenous ER chaperone-protein HSPA5 (Figure 5G and H) or preincubated with

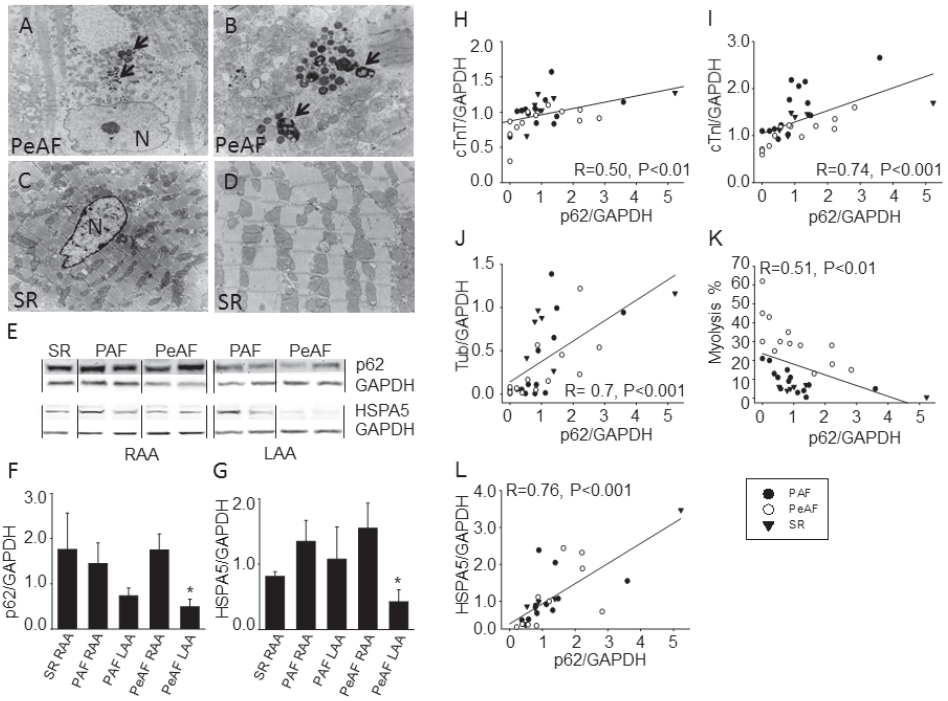

Figure 4 Patients with persistent AF show markers of ER stress and autophagy. A) Electron microscopic image of left atrial appendage of a patient with persistent atrial fibrillation (PeAF), arrows indicate the presence of autophagosomes with a perinuclear (N) localization. **B)** Image of left atrial appendage of a patient with PeAF at a higher magnification, showing the presence of autophagosomes. **C)** Image of left atrial appendage of a patient in sinus rhythm (SR), showing normal sarcomere structures and absence of perinuclear autophagosomes. **D)** Image of left atrial appendage of patient in SR, showing normal sarcomere structures and absence of perinuclear autophagosomes at a higher magnification. **E)** Representative Western blot of the autophagy marker p62 and ER stress marker HSPA5 in right (RAA) and left atrial appendages (LAA) of patients in paroxysmal (PAF) and persistent AF (PeAF) versus SR. **F)** and **G)** Quantified data of autophagy marker p62 and ER stress marker HSPA5 in right (RAA) and left atrial appendages (LAA) of patients with paroxysmal AF (PAF), persistent (PeAF) and control patients in sinus rhythm (SR). *****$P \leq 0.05$ versus SR. **H-L)** Significant correlations between levels of the autophagy marker p62 and markers of cardiomyocyte structural remodeling in patients with paroxysmal (PAF) and persistent (PeAF) and sinus rhythm (SR). **H)** Cardiac troponin T (cTnT), **I)** cardiac troponin I (cTnI), **J)** α-tubulin (tub), **K)** myolysis and **L)** HSPA5.

pepstatin A and BAF for 30 minutes prior to pacing (Figure 5E and F). Pepstatin A and BAF effects are not conveyed via indirect modulation of ER stress, as neither of the drugs influenced HSPA5 expression levels, as suggested before (Figure S5).[34]

To extend these findings to a multicellular experimental animal model for tachypacing-induced contractile dysfunction, similar experiments were conducted in *Drosophila*.[3,35] Comparable to findings in tachypaced HL-1 cardiomyocytes, inhibition of ER stress (4PBA) and autophagy (BAF) attenuates tachypacing-induced dysfunction in heart wall contractions in *Drosophila* (Figure 5I and J), while pepstatin A is not protective and toxic at the concentrations applied.

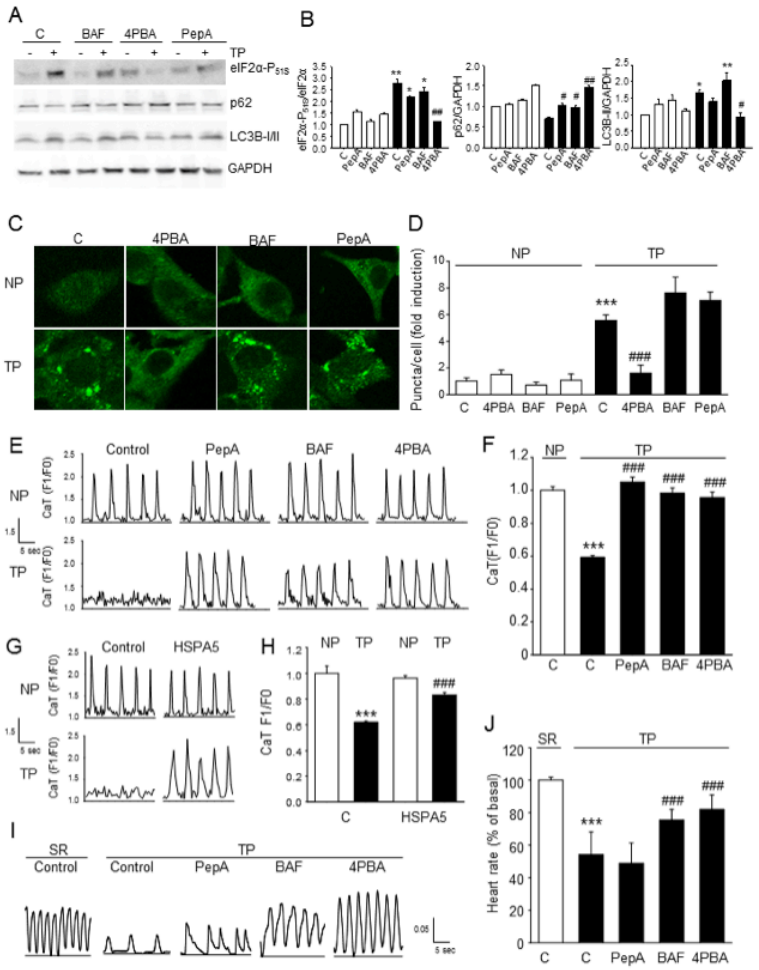

Figure 5 Inhibition of ER stress and autophagy protects against tachypacing-induced contractile dysfunction in HL-1 cardiomyocytes and *Drosophila melanogaster*. A) Representative Western blot of ER stress marker (eIF2α-P51S) and autophagy markers (LC3B and p62) in HL-1 cardiomyocytes pre-treated with DMSO (control) or the autophagy modulators pepstatin A (PepA) or bafilomycin A1 (BAF) or 4PBA. **B)** Quantified data showing that HL-1 cardiomyocytes treated with 4PBA reveal attenuation of tachypacing-induced increase in eIF2α-P51S, LC3B-II induction and reduction in p62. Pepstatin A and bafilomycin A1 inhibit lysosomal cathepsin D/E and lysosomal fusion, respectively, and therefore result in an induction of LC3B-II levels and attenuation of p62 reduction without effecting upstream eIF2α-P51S levels. **C)** Confocal images of normal (NP) and 8h tachypaced (TP) HL-1 cardiomyocytes stained for myosin heavy chain (MHC) with DMSO (Control), or 4PBA, bafilomycin A1 (BAF) or pepstatin A (PepA) pretreatment. **D)** Quantified data showing the number of puncta for the conditions as indicated. 4PBA pretreatment protects against the formation of perinuclear puncta. **E)** Representative CaT of HL-1 cardiomyocytes after normal pacing (NP) or tachypacing (TP). HL-1 cardiomyocytes were pre-treated with the autophagy modulators PepA or BAF or 4PBA, followed by normal or tachypacing and measurement of CaT. **F)** Quantified CaT amplitude of NP and TP HL-1 cardiomyocytes, each from groups as indicated. **G)** Representative CaT of HL-1 cardiomyocytes transfected with empty plasmid (Control) or ER chaperone HSPA5, followed by NP or TP. **H)** Quantified CaT amplitude of NP and TP HL-1 cardiomyocytes transiently transfected with empty plasmid or HSPA5. **I)** Representative heart wall contractions of *Drosophila* monitored before TP and after TP with DMSO (Control) or PepA, BAF or 4PBA pretreatment. **J)** Quantified data showing heart wall contraction rates each from groups as indicated. White bars represent normal paced (NP in HL-1 cardiomyocytes) or spontaneous heart rate (SR in *Drosophila*) and black bars represent tachypaced HL-1 cardiomyocytes or *Drosophila*. N=9 to 15 prepupae for each group. **P*≤0.05, ***P*≤0.01, ****P*≤0.001 vs control NP or SR, #*P*≤0.05, ##*P*≤0.01, ### *P*≤0.001 vs control TP.

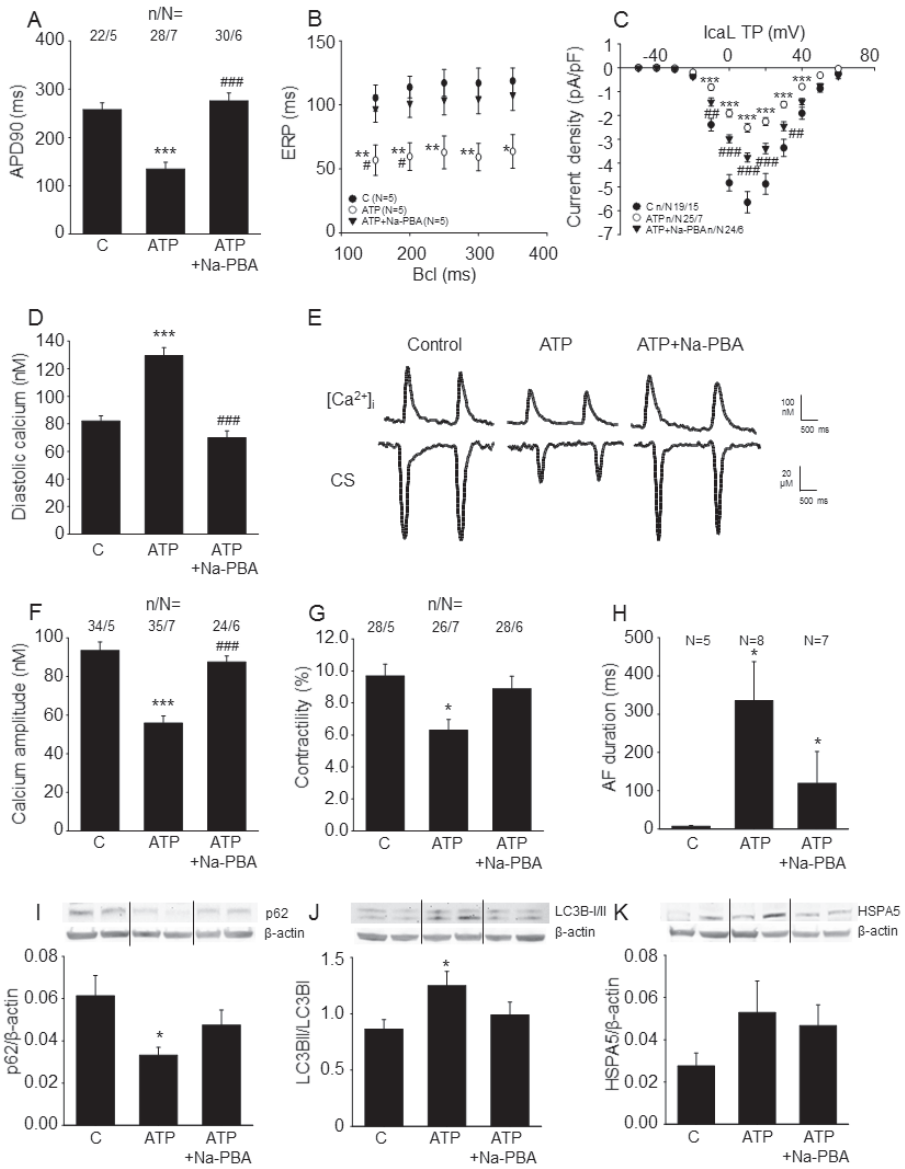

Figure 6 Na-PBA protects against atrial remodeling in a dog model for AF. Atrial tachypacing (ATP) induces atrial remodeling, measured as **A)** shortening of action potential duration (ADP90), **B)** reduced adaptation of the effective refractory period (ERP) at different basic cycle lengths (BCL), **C)** reduced L-type Ca^{2+} current (I_{CaL}) and **D)** increased diastolic calcium levels in cardiomyocytes (n= 15-40 cardiomyocytes). **E)** Representative calcium transient (CaT) and cell shortening (CS) tracers for the conditions as indicated. Furthermore, ATP results in **F)** loss of CaT amplitude, **G)** loss of contractility and **H)** increased duration of induced AF. All ATP-induced atrial remodeling endpoints were significantly attenuated by Na-PBA treatment. **I)** Top panels shows representative Western blot, below quantified data revealing a significant reduction in p62 levels in ATP, which was not significantly reduced by Na-PBA treatment compared to control dogs. **J)** Representative Western blot of LC3B-I/II in groups as indicated. ATP causes significant induction in LC3B-II/I ratio which was not changed in case of Na-PBA treatment. **K)** Representative Western blot of HSPA5 showing a trend (P=0.058) in induction of HSPA5, which was not altered in Na-PBA treated group. *P<0.05, **P≤0.01, ***P≤0.001 versus C, #P<0.05, ##P≤0.01, ###P≤0.001 versus ATP.

Finally, to obtain proof that 4PBA has a beneficial action for an extended time period in a large animal model for AF, dogs subjected to 7 days of atrial tachypacing to induce AF-associated atrial remodeling were treated with the orally-administered sodium-salt PBA (Na-PBA, 300 mg/kg per day). Na-PBA treatment protects not only from tachypacing-induced electrical changes, including shortening of action potential duration, effective refractory period and reductions in L-type Ca^{2+} channel current (Figure 6A-C), but also prevents tachypacing-induced abnormalities in Ca^{2+} handling and associated hypocontractility of isolated atrial cardiomyocytes (Figure 6D-G). The Na-PBA-induced attenuation of adverse electrical and contractile remodeling is associated with a reduction in vulnerability to induce AF by tachypacing (Figure 6H). Finally, Na-PBA reduces markers of ER stress and autophagy in left atrial tissue of tachypaced dogs, as demonstrated by reductions in LC3B-II levels and the increase in p62 levels compared to non-treated tachypaced dogs (Figure 6I and J). ATP resulted in an upward trend in HSPA5 levels and in the presence of Na-PBA no statistically significant changes were seen (Figure 6K). In addition, HDAC activity levels were not altered by Na-PBA treatment, as has been suggested before (Figure S6).[36]

Thus, the inhibition of autophagy protects against tachypacing-induced cardiac remodeling and inhibition of upstream ER stress is sufficient to block activation of autophagy and maintain proper cardiomyocyte function (Figure 7). Findings from a clinically relevant dog model for AF indicate that 4PBA protects the heart against AF, making 4PBA an interesting drug candidate to treat clinical AF.

DISCUSSION

Atrial fibrillation is the most frequent human arrhythmia, displaying an accelerating nature because of progressive remodeling of cardiomyocytes. Current therapies are symptomatic and aim for rate control but do not prevent expansion of the arrhythmogenic substrate.[1] As a consequence, most patients eventually develop permanent AF, which substantially increases cardiac morbidity and mortality and warrants life-long anticoagulant therapy. Despite extensive investigation of the molecular substrate of cardiac remodeling in AF, no effective therapy is available to date. Recently, we proposed that disruption of protein homeostasis contributes importantly to cardiomyocyte remodeling in AF.[3-6] Here, we show in patient atrial tissue and several experimental AF models that AF features an early induction of ER stress, of which effects on cardiac remodeling are mainly conveyed by downstream activation of autophagy. Furthermore, we demonstrate as a "proof-of-concept" that inhibition of ER stress by the orphan drug

4PBA effectively prevents cardiac remodeling in cardiomyocytes, *Drosophila* and dog. The results thus disclose novel druggable targets to limit cardiac remodeling in AF, and propose that 4PBA may emerge as the first effective compound to attenuate AF progression and increase the success rate of cardioversion.

While it is recognized that the increased atrial activation rate constitutes a major driving force for cardiac remodeling in AF,[1] upstream molecular events have been poorly identified. The current data from patients and various models allow for the construction of a comprehensive model featuring ER stress as its most upstream event (Figure 7). Most likely, ER stress results from calcium overload and activation of calmodulin-dependent kinase[37] in response to the high activation rate.[6] During ER stress, HSPA5 dissociates from stress sensors (ATF6, IRE1, PERK) in the ER and recognizes and binds misfolded proteins by their externalized hydrophobic regions. This results in the activation of the unfolded protein response (UPR).[38] The UPR induces the phosphorylation of eIF2α at S51, which inhibits protein translation and initiates selective expression of stress-responsive transcripts, including ATF4 and ATF6.[10] In turn, ATF4 and ATF6 signaling induces CHOP, autophagy gene ATG12, LC3B and HSPA5 expression, thus activating autophagy by stimulating induction and elongation of autophagosomes.[38]. In the current study we found increased HSPA5 expression in HL-1 cardiomyocytes but decreased HSPA5 expression in PeAF patients. The discrepancy between these findings may lie in possible exhaustion of HSPA5 during disease progression in PeAF patients. Finally, during prolonged ER stress, phosphorylated eIF2α replenishes cellular supplies of ATG12, CHOP and LC3B, allowing for sustained and excessive autophagic flux.[26,39-41] Ultimately, autophagy leads to well documented features of cardiac remodeling, including hypertrophy, fibrosis and myolysis.[13,42,43]

In addition to the observed changes in expression and posttranslational modifications of proteins discussed above, specific interventions also support ER stress-induced autophagy in AF. The protection from cardiac dysfunction by inhibitors of autophagy, suggests this route to represent a key effector pathway in tachypacing-induced cardiac remodeling. Indeed, our experiments indicate that autophagy represents the main effector pathway of ER stress, as autophagy inhibitors precluded remodeling without affecting the ER stress response. In agreement, inhibition of ER stress with the chemical chaperone 4PBA or by selective overexpression of HSPA5 suppressed both autophagy and cardiac remodeling. The key role of autophagy in cardiac remodeling, as identified in AF, is supported by other studies. Comparable to our findings, an association between autophagy and the presence of myolysis was reported previously in patients

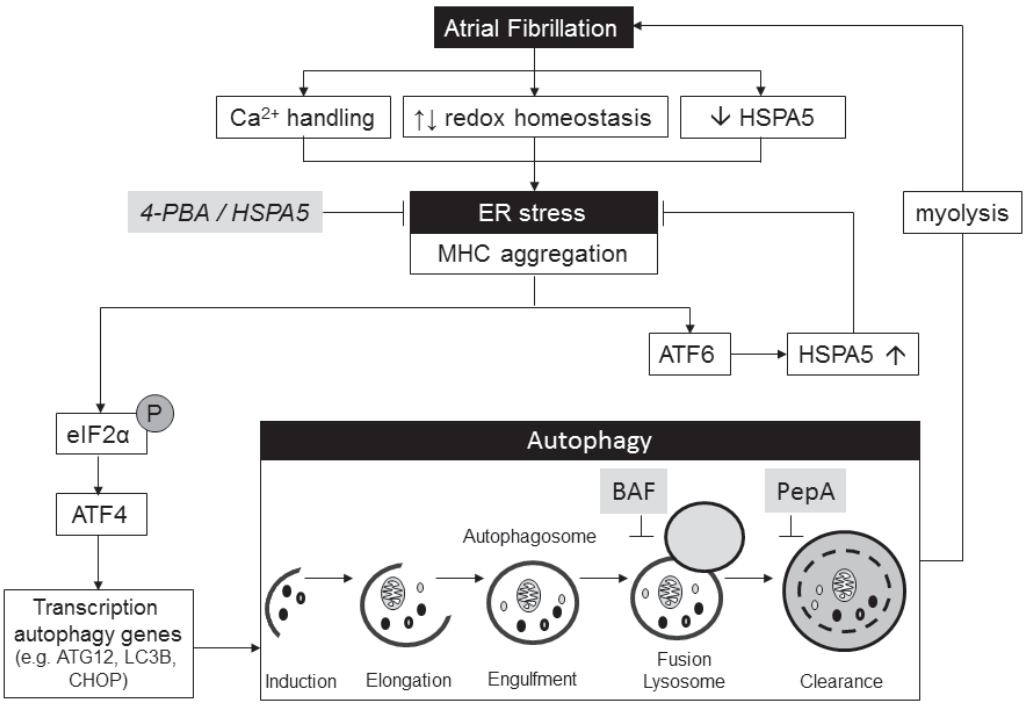

Figure 7 Proposed model for the role of autophagy and disease progression in AF. Starting from the top, AF triggers ER stress in cardiomyocytes through altered Ca^{2+} handling, derailment in redox homeostasis and reduction in ER chaperone HSPA5 levels. This leads to myosin heavy chain (MHC) aggregation and the subsequent ER stress response activates downstream phosphorylation of eIF2α.[51] In turn, this results in the activation of the transcription factor ATF4, which regulates the expression of autophagy genes (ATGs) and LC3B, causing activation of autophagy by stimulating induction and elongation of autophagosomes. A second consequence of the ER stress response results in activation of ATF6, which upregulates the expression of HSPA5 in an attempt to restore ER homeostasis. Initially, AF-induced activation of autophagy may preserve cardiomyocyte proteostasis; however, excessive stress-induced autophagy contributes to loss of contractile function and cardiac remodeling, possibly due to autophagy-induced myolysis. ER stress-induced autophagy appears maladaptive, as inhibition of autophagy via 4PBA, HSPA5 overexpression, pepstatin A (PepA) and bafilomycin A1 (BAF) prevented AF-induced loss of calcium transients.

with mitral regurgitation.[13] Furthermore, an accumulation of autophagosomes was observed in patients who developed post-surgical AF.[44]

From a translational perspective, the current results identify a potential benefit of pharmacological inhibition of autophagy as a therapeutic strategy in clinical AF. It should be noted, however, that effectiveness was only established by pretreatment of tachypacing-induced cardiac changes in the various models. Whether this also applies in humans awaits further confirmation. Moreover, this strategy may only be applicable in specific settings, such as treatment of paroxysmal AF or to prevent post-operative AF induction, but may fail in advanced stages such as (longstanding) persistent AF. Among the available compounds, 4PBA seems highly promising, as this compound

is already approved for clinical use to treat urea cycle disorders,[30,31,45] and available under the trade names Buphenyl (USA as from 1996) and Ammonaps (Europe as from 1999). 4PBA acts as a chemical chaperone and alleviates ER stress by protecting from aggregation of misfolded proteins. With respect to dosing, duration of action and side-effects, much may be learned from outcomes of ongoing human trials with 4PBA, which target various clinical diseases featuring protein misfolding, including Amyotrophic Lateral Sclerosis (NCT00107770), Huntington's disease (NCT00212316), spinal muscular atrophy (NCT00528268), proteinuric nephropathies (NCT02343094) and cystic fibrosis (NCT00016744). Data from patients with urea cycle disorders so far indicate that 4PBA is safe and displays minor side-effects,[29] although conventional dosing is high (max 20 g per day). In addition to 4PBA, our results indicate that cardiac remodeling in AF may also be modulated by inhibitors of autophagy.[39,46,47] However, treatment with autophagy inhibitors may precipitate considerable toxicity, as reported for bafilomycin,[48] or additional detrimental effects because of disruption of normal cell physiology by inhibition of basal autophagy.[12,14,49,50] Application of inhibitors of autophagy in AF and other chronic conditions thus awaits development of selective inhibitors targeting excessive autophagy. Because of these considerations, 4PBA currently represents the best candidate to explore the benefits of repression of autophagy in the attenuation of AF progression and improvement of cardioversion outcome in clinical AF.

Funding

This study was supported by the Dutch Heart Foundation (2007B217, 2009B024, 2013T096, 2013T144), LSH-Impulse grant (40-43100-98-008), NWO VICI grant (865.10.012 to Dr. Sibon), the Canadian Institutes of Health Research (grant #6957) and the Quebec Heart and Stroke Foundation.

References

1. Dobrev D, Carlsson L, Nattel S. Novel molecular targets for atrial fibrillation therapy. *Nat Rev Drug Discov*. 2012;11(4):275-291.

2. de Groot NM, Houben RP, Smeets JL, et al. Electropathological substrate of longstanding persistent atrial fibrillation in patients with structural heart disease: Epicardial breakthrough. *Circulation*. 2010;122(17):1674-1682.

3. Zhang D, Wu CT, Qi X, et al. Activation of histone deacetylase-6 induces contractile dysfunction through derailment of alpha-tubulin proteostasis in experimental and human atrial fibrillation. *Circulation*. 2014;129(3):346-358.

4. Brundel BJ, Ausma J, van Gelder IC, et al. Activation of proteolysis by calpains and structural changes in human paroxysmal and persistent atrial fibrillation. *Cardiovasc Res*. 2002;54(2):380-389.

5. Ausma J, van der Velden HM, Lenders MH, et al. Reverse structural and gap-junctional remodeling after prolonged atrial fibrillation in the goat. *Circulation*. 2003;107(15):2051-2058.

6. Qi XY, Yeh YH, Xiao L, et al. Cellular signaling underlying atrial tachycardia remodeling of L-type calcium current. *Circ Res*. 2008;103(8):845-854.

7. Ke L, Qi XY, Dijkhuis AJ, et al. Calpain mediates cardiac troponin degradation and contractile dysfunction in atrial fibrillation. *J Mol Cell Cardiol*. 2008;45(5):685-693.

8. Brundel BJ, Shiroshita-Takeshita A, Qi X, et al. Induction of heat shock response protects the heart against atrial fibrillation. *Circ Res*. 2006;99(12):1394-1402.

9. Ke L, Meijering RA, Hoogstra-Berends F, et al. HSPB1, HSPB6, HSPB7 and HSPB8 protect against RhoA GTPase-induced remodeling in tachypaced atrial myocytes. *PLoS One*. 2011;6(6):e20395.

10. Kroemer G, Marino G, Levine B. Autophagy and the integrated stress response. *Mol Cell*. 2010;40(2):280-293.

11. Yang Z, Klionsky DJ. Eaten alive: A history of macroautophagy. *Nat Cell Biol*. 2010;12(9):814-822.

12. Nakai A, Yamaguchi O, Takeda T, et al. The role of autophagy in cardiomyocytes in the basal state and in response to hemodynamic stress. *Nat Med*. 2007;13(5):619-624.

13. Chen MC, Chang JP, Wang YH, Liu WH, Ho WC, Chang HW. Autophagy as a mechanism for myolysis of cardiomyocytes in mitral regurgitation. *Eur J Clin Invest*. 2011;41(3):299-307.

14. Gurusamy N, Das DK. Is autophagy a double-edged sword for the heart? *Acta Physiol Hung*. 2009;96(3):267-276.

15. Zhu H, Tannous P, Johnstone JL, et al. Cardiac autophagy is a maladaptive response to hemodynamic stress. *J Clin Invest*. 2007;117(7):1782-1793.

16. Claycomb WC, Lanson NA,Jr, Stallworth BS, et al. HL-1 cells: A cardiac muscle cell line that contracts and retains phenotypic characteristics of the adult cardiomyocyte. *Proc Natl Acad Sci U S A*. 1998;95(6):2979-2984.

17. Pankiv S, Clausen TH, Lamark T, et al. p62/SQSTM1 binds directly to Atg8/LC3 to facilitate degradation of ubiquitinated protein aggregates by autophagy. *J Biol Chem*. 2007;282(33):24131-24145.

18. Grynkiewicz G, Poenie M, Tsien RY. A new generation of Ca^{2+} indicators with greatly improved fluorescence properties. *J Biol Chem*. 1985;260(6):3440-3450.

19. Wang QJ, Ding Y, Kohtz DS, et al. Induction of autophagy in axonal dystrophy and degeneration. *J Neurosci*. 2006;26(31):8057-8068.

20. Maejima Y, Kyoi S, Zhai P, et al. Mst1 inhibits autophagy by promoting the interaction between Beclin1 and bcl-2. *Nat Med*. 2013;19(11):1478-1488.

21. Gottlieb RA, Mentzer RM. Autophagy during cardiac stress: Joys and frustrations of autophagy. *Annu Rev Physiol*. 2010;72:45-59.

22. Hansen TE, Johansen T. Following autophagy step by step. *BMC Biol*. 2011;9:39-7007-9-39.

23. Gurusamy N, Das DK. Detection of cell death by autophagy. *Methods Mol Biol*. 2009;559:95-103.

24. Jung CH, Ro SH, Cao J, Otto NM, Kim DH. mTOR regulation of autophagy. *FEBS Lett*. 2010;584(7):1287-1295.

25. Yung HW, Charnock-Jones DS, Burton GJ. Regulation of Akt phosphorylation at Ser473 and Thr308 by endoplasmic reticulum stress modulates substrate specificity in a severity dependent manner. *PLoS One*. 2011;6(3):e17894.

26. Kouroku Y, Fujita E, Tanida I, et al. ER stress (PERK/eIF2alpha phosphorylation) mediates the polyglutamine-induced LC3 conversion, an essential step for autophagy formation. *Cell Death Differ*. 2007;14(2):230-239.

27. Li D, Shinagawa K, Pang L, et al. Effects of angiotensin-converting enzyme inhibition on the development of the atrial fibrillation substrate in dogs with ventricular tachypacing-induced congestive heart failure. *Circulation*. 2001;104(21):2608-2614.

28. Voigt N, Trausch A, Knaut M, et al. Left-to-right atrial inward rectifier potassium current gradients in patients with paroxysmal versus chronic atrial fibrillation. *Circ Arrhythm Electrophysiol*. 2010;3(5):472-480.

29. Carducci MA, Gilbert J, Bowling MK, et al. A phase I clinical and pharmacological evaluation of sodium phenylbutyrate on an 120-h infusion schedule. *Clin Cancer Res*. 2001;7(10):3047-3055.

30. Kibleur Y, Dobbelaere D, Barth M, Brassier A, Guffon N. Results from a nationwide cohort temporary utilization authorization (ATU) survey of patients in france treated with pheburane (A (R)) (sodium phenylbutyrate) taste-masked granules. *Paediatr Drugs*. 2014;16(5):407-415.

31. Berry SA, Lichter-Konecki U, Diaz GA, et al. Glycerol phenylbutyrate treatment in children with urea cycle disorders: Pooled analysis of short- and long-term ammonia control and outcomes. *Mol Genet Metab*. 2014;112(1):17-24.

32. Kolb PS, Ayaub EA, Zhou W, Yum V, Dickhout JG, Ask K. The therapeutic effects of 4-phenylbutyric acid in maintaining proteostasis. *Int J Biochem Cell Biol*. 2015;61:45-52.

33. Cuadrado-Tejedor M, Ricobaraza AL, Torrijo R, Franco R, Garcia-Osta A. Phenylbutyrate is a multifaceted drug that exerts neuroprotective effects and reverses the Alzheimer's disease-like phenotype of a commonly used mouse model. *Curr Pharm Des*. 2013;19(28):5076-5084.

34. Ryter SW, Cloonan SM, Choi AM. Autophagy: A critical regulator of cellular metabolism and homeostasis. *Mol Cells*. 2013;36(1):7-16.

35. Zhang D, Ke L, Mackovicova K, et al. Effects of different small HSPB members on contractile dysfunction and structural changes in a drosophila melanogaster model for atrial fibrillation. *J Mol Cell Cardiol*. 2011;51(3):381-389.

36. Mimori S, Ohtaka H, Koshikawa Y, et al. 4-phenylbutyric acid protects against neuronal cell death by primarily acting as a chemical chaperone rather than histone deacetylase inhibitor. *Bioorg Med Chem Lett*. 2013;23(21):6015-6018.

37. Nishida K, Kyoi S, Yamaguchi O, Sadoshima J, Otsu K. The role of autophagy in the heart. *Cell Death Differ*. 2009;16(1):31-38.

38. Rashid HO, Yadav RK, Kim HR, Chae HJ. ER stress: Autophagy induction, inhibition and selection. *Autophagy*. 2015;11(11):1956-1977.

39. Fleming A, Noda T, Yoshimori T, Rubinsztein DC. Chemical modulators of autophagy as biological probes and potential therapeutics. *Nat Chem Biol*. 2011;7(1):9-17.

40. Verfaillie T, Salazar M, Velasco G, Agostinis P. Linking ER stress to autophagy: Potential implications for cancer therapy. *Int J Cell Biol*. 2010;2010:930509.

41. Hayashi-Nishino M, Fujita N, Noda T, Yamaguchi A, Yoshimori T, Yamamoto A. A subdomain of the endoplasmic reticulum forms a cradle for autophagosome formation. *Nat Cell Biol*. 2009;11(12):1433-1437.

42. Ghavami S, Cunnington RH, Gupta S, et al. Autophagy is a regulator of TGF-beta1-

induced fibrogenesis in primary human atrial myofibroblasts. *Cell Death Dis*. 2015;6:e1696.

43. Tham YK, Bernardo BC, Ooi JY, Weeks KL, McMullen JR. Pathophysiology of cardiac hypertrophy and heart failure: Signaling pathways and novel therapeutic targets. *Arch Toxicol*. 2015;89(9):1401-1438.

44. Garcia L, Verdejo HE, Kuzmicic J, et al. Impaired cardiac autophagy in patients developing postoperative atrial fibrillation. *J Thorac Cardiovasc Surg*. 2012;143(2):451-459.

45. Schonthal AH. Targeting endoplasmic reticulum stress for cancer therapy. *Front Biosci (Schol Ed)*. 2012;4:412-431.

46. Balgi AD, Fonseca BD, Donohue E, et al. Screen for chemical modulators of autophagy reveals novel therapeutic inhibitors of mTORC1 signaling. *PLoS One*. 2009;4(9):e7124.

47. Sciarretta S, Zhai P, Volpe M, Sadoshima J. Pharmacological modulation of autophagy during cardiac stress. *J Cardiovasc Pharmacol*. 2012;60(3):235-241.

48. Drose S, Altendorf K. Bafilomycins and concanamycins as inhibitors of V-ATPases and P-ATPases. *J Exp Biol*. 1997;200(Pt 1):1-8.

49. Maruyama R, Goto K, Takemura G, et al. Morphological and biochemical characterization of basal and starvation-induced autophagy in isolated adult rat cardiomyocytes. *Am J Physiol Heart Circ Physiol*. 2008;295(4):H1599-607.

50. Hara T, Nakamura K, Matsui M, et al. Suppression of basal autophagy in neural cells causes neurodegenerative disease in mice. *Nature*. 2006;441(7095):885-889.

51. Hetz C, Chevet E, Oakes SA. Proteostasis control by the unfolded protein response. *Nat Cell Biol*. 2015;17(7):829-838.

SUPPLEMENTAL FIGURES

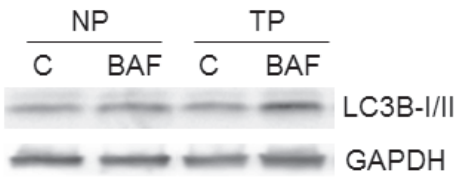

Figure S1 BAF treatment further increases LC3B-II levels in tachypaced HL-1 cardiomyocytes. Representative Western blot showing LC3B-I/II expression in normal paced (NP) and tachypaced (TP) HL-1 cardiomyocytes with and without BAF treatment. BAF increases the LC3B-II levels after 8h tachypacing.

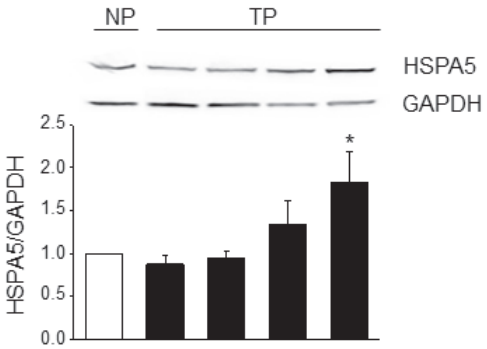

Figure S2 Tachypacing induces expression of the ER chaperone HSPA5. Top panel: representative Western blot showing HSPA5 and GAPDH expression in normal paced (NP) and tachypaced (TP) HL-1 cardiomyocytes. Bottom: quantified data revealing significant increase in HSPA5 levels in tachypaced HL-1 cardiomyocytes. *$P \leq 0.05$ vs NP.

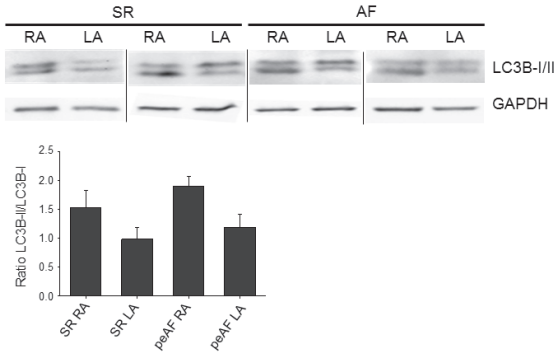

Figure S3 LC3B-I/II levels show borderline significant changes in patients with persistent AF compared to control patients in sinus rhythm. Top panel: representative Western blot showing LC3B-I, LC3B-II and GAPDH levels in right atrial appendages (RA) and left atrial appendages (LA) of patients with persistent AF (PeAF) or control patients in sinus rhythm (SR). Lower panel: quantified data showing a borderline significant induction (P=0.06) of LC3B-II/I ratio in RA of patients with PeAF compared to RA of SR.

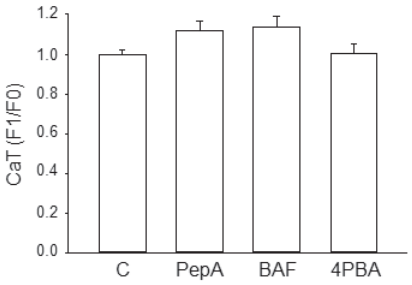

Figure S4 Pharmacological modulation of autophagy in normal-paced HL-1 cardiomyocytes does not change calcium transients. Quantified CaT of HL-1 cardiomyocytes pretreated with autophagy modulators pepstatin A or bafilomycin A1 or 4PBA and subjected to normal pacing. CaT of tachypaced HL-1 cardiomyocytes are presented in Figure 5D.

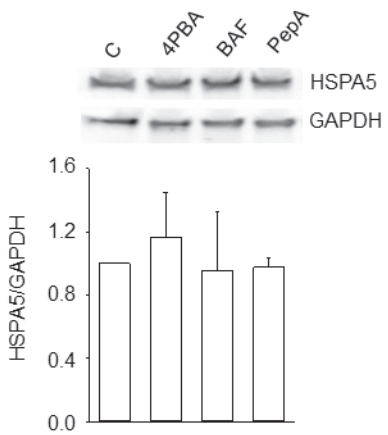

Figure S5 Pharmacological modulation of autophagy in HL-1 cardiomyocytes does not change HSPA5 expression. Top panel: representative Western blot showing HSPA5 and GAPDH levels in HL-1 cardiomyocytes pretreated with various autophagy modulators as indicated. Lower panel: quantified data showing no significant changes in HSPA5 levels for the conditions as indicated.

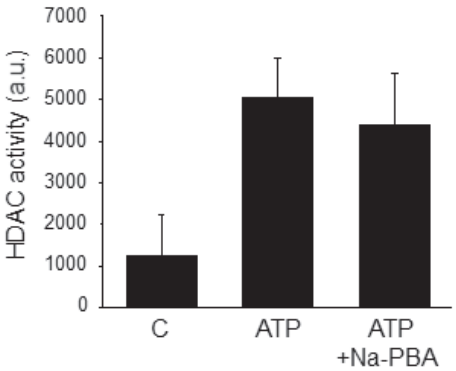

Figure S6 4PBA has no effect on HDAC activity in dogs. Atrial tachypacing of dogs results in a borderline significant induction (*P*=0.06) of HDAC activity, which was not altered by 4PBA treatment.